JOURNAL OF RESEARCH of the National Bureau of Standards—A. Physics and Chemistry
Vol. 74A, No. 2, March–April 1970

Photoelastic Constants of Ruby*

R. M. Waxler and E. N. Farabaugh

Institute for Materials Research, National Bureau of Standards, Washington, D.C. 20234

(October 21, 1969)

The eight piezo-optic and eight elasto-optic constants of synthetic, single crystal ruby have been determined using the cadmium red radiation of 643.8 nanometers (nm). All the constants are found to be negative in value, or to have very small positive values. The data indicate that changes in the polarizability of the oxygen ion and changes in the local field are primarily responsible for the observed changes in refractive index. Hydrostatic pressure has been used for the first time as part of a complete photoelastic investigation, and a new, screw-clamp device for easily attaining high, uniaxial stress is described.

Key words: Birefringence; crystals, lasers; photoelasticity; ruby.

1. Introduction

Thermo-optic and piezo-optic data on ruby are of interest in laser technology because of the large temperature and stress gradients created in a laser solid. The induced changes in refractive index play a large part in the distortion of the wavefront of the light generated [1].[1] Houston et. al., have reported on the change in refractive index of ruby from −180 to 70 °C [2]. Mandarino [3] has reported on the birefringence introduced into a ruby crystal by loading along the c axis, and there are some data in the literature on the photoelastic constants of sapphire [4, 5, 6, 7]. In view of the widespread use of ruby as a laser material, it was felt that a complete investigation of its photoelastic properties was appropriate.

2. Theoretical Considerations

Ruby belongs to the $\bar{3}$m point group of the trigonal system, and a sterographic projection showing the symmetry elements of this point group is presented in figure 1. In the figure, the open triangle represents the $\bar{3}$ axis, the diad symbols represent 2-fold axes, and the heavy lines indicate mirror planes. The right-handed coordinate system $x_1x_2x_3$ used to specify the photoelastic constants [8, 9] together with the corresponding hexagonal Miller-Bravais indices are also shown. Measurements made on ruby at 643.8 nm show that the refractive index of the ordinary ray, $n_\omega = 1.76569$, and the refractive index of the extraordinary ray, $n_\epsilon = 1.75759$ [10]. The refractive index ellipsoid is, therefore, an ellipsoid of revolution where the axis of infinite rotation coincides with the unique, x_3 axis of the crystal. According to Neumann's principle, the point group symmetry of the index ellipsoid, ∞/mm, must include the $\bar{3}$m symmetry of the ruby [8].

Curie's principle states that the symmetry elements common to the point group of the unstressed crystal and to the point group of the stress give the point group of the stressed crystal [8, 11, 12]. Applied hydrostatic pressure has spherical symmetry, ∞ ∞ m, and a uniaxial stress has the symmetry ∞/mm. Therefore, the symmetry elements of the index ellipsoid of ruby will not be altered if hydrostatic pressure is applied, or if a uniaxial stress is applied along the unique, x_3 axis shown in figure 1. If a uniaxial stress is applied along x_1 shown in figure 1, the 2-fold axis of rotation along the line of stress is the only symmetry element which will be retained. The refractive index ellipsoid will become triaxial; one principal radius will be pinned along the 2-fold axis, and the other two principal radii will be free to rotate in the x_2x_3 plane. If a uniaxial stress is imposed along x_2, again the 2-fold rotation axis along x_1 is the only symmetry element that is retained, and one principal direction of the ellipsoid is fixed in this direction. The other two principal radii are free to rotate in the mirror plane, as before, but now they will rotate in the opposite sense. In general, when a uniaxial stress is applied along any line lying in the x_2x_3 plane, one principal radius of the index ellipsoid will coincide with x_1, and the other two radii will lie in the x_2x_3 plane.

Ruby has eight piezo-optic constants, q_{11}, q_{12}, q_{13}, q_{14}, q_{31}, q_{33}, q_{41}, q_{44}, and eight elasto-optic constants, p_{11}, p_{12}, p_{13}, p_{14}, p_{31}, p_{33}, p_{41}, p_{44}. According to Pockels theory, when a stress, P_j is applied, the induced changes in the relative dielectric impermeability, $\mathbf{B}$ ($\mathbf{B} \equiv \mathbf{n}^{-2}$) is $\Delta B_i = q_{ij}P_j$ $i, j = 1$ to 6. Similar

*Research partially supported by the Advanced Research Projects Agency of the Department of Defense.

[1] Figures in brackets indicate the literature references at the end of this paper.

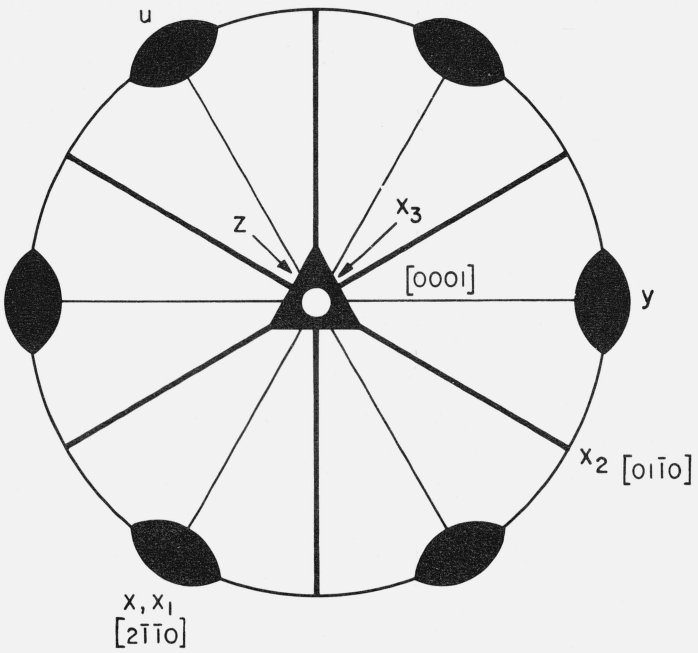

FIGURE 1. *Stereogram of point group 3m.*

$x_1x_2x_3$ represent the principal vibration directions of the refractive index ellipsoid. xyuz is the Miller-Bravais coordinate system.

relations hold between ΔB_i, p_{ij} and the strain components. The two sets of constants are related by

$$p_{ij} = \sum_{k=1}^{6} q_{ik} c_{kj} \tag{1}$$

and

$$q_{ij} = \sum_{k=1}^{6} p_{ik} s_{kj}, \tag{2}$$

where the c's and s's are respectively the elastic constants and elastic compliances [8].

3. Experimental Procedure

The general experimental approach is to stress the specimen either by uniaxial loading or applied hydrostatic pressure and then to measure the absolute changes in optical path length or the changes in optical path difference. By choosing different crystallographic directions for loading and different directions for light beam propagation, sufficient simultaneous equations can be obtained to evaluate all of q_{ij} and p_{ij}.

3.1. Preparation of Specimens

The single crystal ruby was obtained commercially in the form of a boule about 20 cm long and 3 cm in diameter. This was a Czochralski grown crystal where the optic axis made an angle of 60° with the axis of the boule. Spectrophotometric analysis indicated that the Cr_2O_3 content was 0.050 percent by weight.

Plates about 0.6 cm thick were cut with a diamond saw from an inclusion free region of the boule so that their surfaces contained the x_2x_3 plane. These plates were then ground on a surface grinder and polished on a lead lap using 4 to 8 μm diamond paste. The specimens, in the form of rectangular prisms, were cut from the plates, and the newly cut surfaces of the prisms, excluding the ends were then ground and polished.

Dimensions of the 6 prisms used for the measurements are given in table 1. The specimens all had a thickness parallel to x_1 and lengths parallel respectively to x_2, x_3, M and M' (see table 1). Using the morphological unit cell of ruby, the orientation of all specimens was accomplished by means of the Laue back-reflection x-ray technique. It should be pointed out that it is possible to distinguish between opposite ends of the 2-fold axes, and this distinction is important because the sign of the piezo-optic constants, q_{14} and q_{41} depends on which end of an axis is considered as being positive. In the present study, the convention used by Wachtman in his investigation of the elastic constants of corundum was followed [9].

In photoelastic studies, it is important that the distribution of stress be uniform in the specimen. This condition is automatically satisfied when hydrostatic pressure is applied. In applying uniaxial compression, care must be taken that the length which is also the direction of stress in the specimen be at least three times the breadth or the thickness, and that the measurements be confined to the middle portion of the specimen [13, 14]. It can be seen in table 1 that two of the prisms do not quite meet these specifications. However, when loading in compression, steel caps were placed on the ends of the specimens so that, in each case, the prism length was adequate (see sec. 3.3).

3.2. Optical Measurements

The prisms were ground and polished so that localized Fizeau-type optical interference fringes could be observed between opposite faces. Measurement of the shift in these fringes with applied stress was used to determine the absolute change in optical path length. This technique was used both for uniaxial loading [13] and applied hydrostatic pressure [15, 6]. The fringes were viewed in reflection using collimated cadmium red light of 643.8 nm at normal incidence. Use was made of a Pulfrich-type viewer which has been greatly

TABLE 1. *Dimensions of rectangular prisms*

Prism No.	Length		Breadth		Thickness	
	mm	Parallel to	mm	Parallel to	mm	Parallel to
1	27.010	x_3	9.880	x_2	8.747	x_1
2	17.850	x_3	6.510	x_2	6.388	x_1
3	31.387	x_2	5.905	x_3	5.482	x_1
4	27.851	x_2	5.894	x_3	5.580	x_1
5	24.461	x_2	5.908	x_3	5.710	x_1
6	31.463	M[a]	5.885	M'	5.648	x_1
7	17.172	M'[b]	5.330	M	5.665	x_1

[a] M indicates the direction equally inclined to x_2 and x_3 and lying in the x_2x_3 plane.
[b] M' indicates the direction equally inclined to $-x_2$ and x_3 and lying in the x_2x_3 plane.

improved by Saunders [16], and, in each experiment, a sheet of polaroid was employed to isolate changes along each of the two principal vibration directions in the crystal.

The change in optical path difference induced by uniaxial loading was also measured. In this case, the specimen was placed in a 45 degree position between crossed nicol prisms, and the relative retardation was measured with a Soleil-Babinet compensator [13].

Since in each experiment, the change in optical path length or induced optical path difference was measured, it was necessary to know the change in thickness of the specimen in order to calculate the changes in refractive index. For this purpose, the elastic constants of corundum determined by Wachtman were employed [9]. The elastic constants of corundum are the same as those of ruby within the experimental error [17].

3.3. Stressing Apparatus and Techniques

For the present problem, three different stressing apparatus were employed: (a) a hydrostatic pressure vessel, (b) a dead weight compression apparatus, and (c) a rectangular frame screw clamp.

a. Hydrostatic Pressure Vessel

For attaining hydrostatic pressures up to 1000 bars a pressure vessel equipped with glass windows was used [15]. The specimen was immersed in a highly transparent mineral oil, and hydrostatic pressure was generated by compressing the oil. In order to increase the visibility of the fringes, the specimen was fully coated with aluminum on the rear reflecting surface, and given a partial coating on the front surface. The shift of the Fizeau-type fringes past a fixed reference mark was observed visually using Saunders' viewer [16]. This technique was used to find the change in refractive index with hydrostatic pressure of the ordinary and extraordinary ray of ruby.

b. Dead Weight Compression Apparatus

A loading frame was used where a yoke with suspended weights brings a piston to bear on the specimen [14]. To insure uniformity of loading, steel caps were fabricated to fit over each end of the specimen. A small depression was machined in both the center of the cap and the center of the piston to accommodate a steel ball at the point of contact. Six calibrated 50-lb weights were used so that the total load was 300 lbs. The dead weight compression apparatus was always used in conjunction with the Soleil-Babinet compensator to determine changes in the relative retardation with a sensitivity of 1×10^{-7}. The pressures attained were of the order of 200 bars yielding data to three significant figures.

c. Rectangular Frame Screw Clamp

A special clamp was made for the purpose of easily attaining compressive stresses up to 10,000 bars. This is shown in figure 2. The screw clamp was used in conjunction with Saunders' viewing apparatus [16] to observe the shift in Fizeau-type interference fringes with load. With this technique, it is possible to note a shift of 0.1 fringe which is equivalent to a change of about 1×10^{-5} in refractive index. It was desirable to attain stresses high enough to induce a reasonably large and measurable shift of Fizeau fringes. Calculations indicated that reliable data on changes of refractive index in the fourth and fifth decimal place could be obtained by stressing to about 1,500 bars.

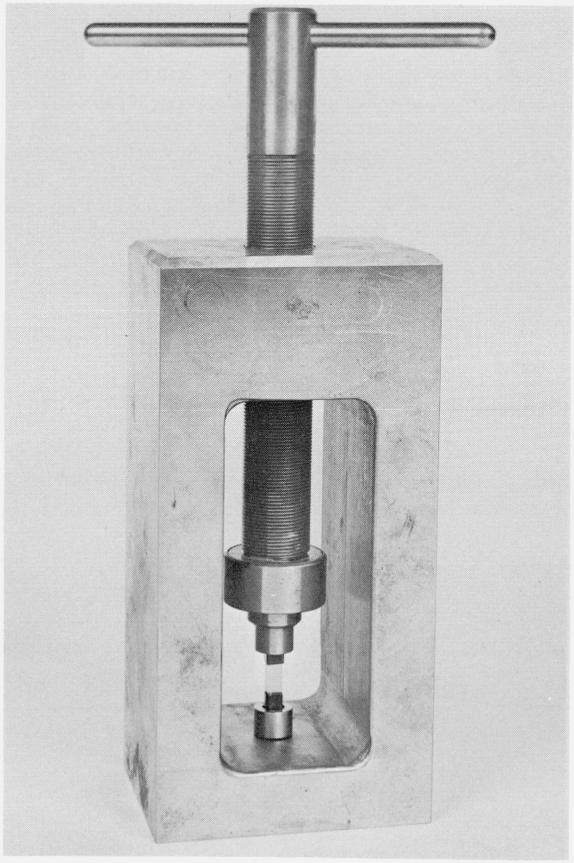

FIGURE 2. *Rectangular frame screw clamp with specimen in place.*

It can be seen in figure 2 that the thrust in the clamp is obtained from a screw which threads in to one end of the block. The screw is 1 inch in diameter, has 20 threads per inch and is built with a thrust bearing at the front so that the specimen is torque free. To insure uniformity of load on the specimen, the technique of using steel caps with steel balls to transmit the stress was employed here as in the dead weight loading apparatus.

In conducting the experiments, the specimen was first placed in the dead weight loading apparatus and the relationship between load and induced double refraction was determined. For ruby, there is evidence to indicate that this relationship is linear to pressures much greater than 200 bars [6]. Having established this linear relationship, the specimen served as its own stress gage when placed in the screw clamp.

The stress was measured by noting the change in the double refraction of the specimen as it was compressed. The absolute change in optical path length for a principal vibration direction was measured by noting the shift in the Fizeau fringes as this stress was released. Using this technique, repeated measurements agreed to within ± 0.1 of a Fizeau fringe.

In the foregoing, a known amount of double-refraction was introduced into the specimen in the following manner. Ordinarily, one pattern of Fizeau fringes could be seen when the E-vector of the polaroid was parallel to the direction of stress, and a second pattern was observable when the E-vector was perpendicular to the stress direction. These two patterns could be made to coincide by adjusting the compressive stress so that the difference in path length between the two vibration directions was some integral number of whole wavelengths. By removing the polaroid from the optical train and slowly turning the screw, the observed pattern of fringes could be made, alternately, to appear and disappear. The fringes disappeared when the optical path length between the two principal vibration directions was an odd number of half wavelengths. By adjusting to a position of complete fringe extinction, two different settings of the screw could be selected so that, in the interval between, a known number of whole wavelengths of optical path difference had been introduced into the specimen.

4. Results and Discussion

The method of calculating the photoelastic constants from the observed change in optical path length has been amply treated by Narasimhamurty [18] and Vedam [19, 13], and will not be given here. The paper by Narasimhamurty on the photoelastic constants of α-quartz is particularly pertinent to the present work because α-quartz and ruby both belong to the seventh Laue-symmetry group and the number of photoelastic constants is the same for both groups. The experimental results are presented in table 2, where the observed path retardation, δ_0, has been reported in

TABLE 2. *Optical path retardation in ruby*

Prism No.	Direction of stress	Direction of observation	Nature of observation	Expression for path retardation, δ_0	Measured value of path retardation, δ_0, cm^2/dyn $\times 10^{13}$
1	x_3	x_1	Relative	$1/2(n_3^3 q_{33} - n_2^3 q_{13}) - s_{13}(n_3 - n_2)$	-1.475
2	x_3	x_1	Absolute (P)	$n_3^3 q_{33} - 2n_3 s_{13}$	$-.98$
2	x_3	x_1	Absolute (N)	$n_2^3 q_{13} - 2n_2 s_{13}$	1.97
3	x_2	x_1	Relative	$1/2(n_2^3 q_{11} - n_3^3 q_{31}) - s_{12}(n_2 - n_3)$	-1.469
4	x_2	x_1	Absolute (P)	$n_2^3 q_{11} - 2n_2 s_{12}$	$-.25$
4	x_2	x_1	Absolute (N)	$n^3 q_{31} - 2n_3 s_{12}$	2.85
3	x_2	x_3	Relative	$1/2n_2^3 (q_{11} - q_{12})$	-1.582
5	x_2	x_3	Absolute (P)	$n_2^3 q_{11} - 2n_2 s_{13}$	-1.55
5	x_2	x_3	Absolute (N)	$n_1^3 q_{12} - 2n_1 s_{13}$	1.62
6	M	M'	Relative	$1/8n_{23}^3(q_{11}+q_{13}-q_{14}+q_{31}+q_{33}+2q_{44}-2q_{41})$ $-1/4n_1^3(q_{12}+q_{13}+q_{14})$ $-1/4(n_{23}-n_1)(s_{11}+2s_{13}+s_{33}-s_{44})$	-1.654
6	M	M'	Absolute (P)	$1/4n_{23}^3(q_{11}+q_{13}-q_{14}+q_{31}+q_{33}+2q_{44}-2q_{41})$ $-1/2n_{23}(s_{11}+2s_{13}+s_{33}-s_{44})$	$-.08$
6	M	M'	Absolute (N)	$1/2n_1^3(q_{12}+q_{13}+q_{14})$ $-1/2n_1(s_{11}+2s_{13}+s_{33}-s_{44})$	3.22
7	M'	M	Relative	$1/8n_{23}^3(q_{11}+q_{13}+q_{14}+q_{31}+q_{33}+2q_{44}+2q_{41})$ $-1/4n_1^3(q_{12}+q_{13}-q_{14})$ $-1/4(n_{23}-n_1)(s_{11}+2s_{13}+s_{33}-s_{44})$	-1.974
7	M'	M	Absolute (P)	$1/4n_{23}^3(q_{11}+q_{13}+q_{14}+q_{31}+q_{33}+2q_{44}+2q_{41})$ $-1/2n_{23}(s_{11}+2s_{13}+s_{33}-s_{44})$	$-.39$
7	M'	M	Absolute (N)	$1/2n_1^3(q_{12}+q_{13}-q_{14})$ $-1/2n_1(s_{11}+2s_{13}+s_{33}-s_{44})$	3.55
2	Hydrostatic pressure	x_1	Absolute	$n_3^3(2q_{31}+q_{33})-2n_3(s_{11}+s_{12}+s_{13})$ (for vibrations parallel to the optic axis)	-6.63
2	Hydrostatic pressure	x_1	Absolute	$n_2^3(q_{11}+q_{12}+q_{13})-2n_2(s_{11}+s_{12}+s_{13})$ (for vibrations perpendicular to the optic axis)	-6.62

centimeters per centimeter thickness of the specimen per unit stress of 1 dyn/cm^2. The measured values of δ_0 reported in the last column represent the combined effect of change in refractive index and dimensional change. It should be noted that the relative values of δ_0 hold for a light beam traversing the specimen only once, and the absolute values pertain for a double passage of the specimen [18, 19]. The (P) and the (N) indicate measurements made with the principal vibration directions, parallel and perpendicular, respectively, to the direction of applied stress. For the different directions of loading and light propagation, theoretical expressions for δ_0 are presented in the next to last column.

Although the principal vibration directions are free to rotate in the x_2x_3 plane when stress is applied along x_2, preliminary calculations indicated that this rotation was extremely small, on the order of 0.02 circular degrees. This slight rotation was neglected, and data obtained from prisms No. 3 and 4 (see table 2) were treated as if there were no rotation at all.

Values of the s_{ij} were taken from Wachtman's paper [9] and inserted into the equations of table 2. Of the resulting 17 simultaneous equations, a computerized least-squares fit was made and the resulting q_{ij} are reported in table 3. The standard deviation of each q_{ij} was 0.02×10^{-13} cm^2/dyn or less. The p_{ij} were then computed from eq (1) and the results are given in table 3.

Mandarino [3] has reported that $(q_{33}-q_{13})=+0.697\times10^{-13}$ cm^2/dyn for ruby with 0.11 percent Cr_2O_3. Our results indicate a negative value, $(q_{33}-q_{13})=-0.54\times10^{-13}$ cm^2/dyn.

Where comparison is possible the photoelastic properties of ruby are found to be close to those of sapphire. Subjecting ruby prism No. 2 to hydrostatic pressure, it was found that the change in refractive index was -1.1×10^{-4}/Kilobar for both the ordinary and extraordinary ray. This agrees within the experimental error with the results of Davis and Vedam on sapphire [6], where they report that $\Delta n_\omega=(-1.0\pm0.2)\times10^{-4}$/Kilobar and $\Delta n_\epsilon=(-1.1\pm0.2)\times10^{-4}$/kilobar.[2]

TABLE 3. *Piezo-optic and elasto-optic constants of ruby*

	Present work	Dixon
q_{11}	−0.52	—
q_{12}	.08	—
q_{13}	.13	—
q_{14}	−.07	—
q_{31}	.01	—
q_{33}	−.41	—
q_{41}	−.01	—
q_{44}	−.71	—
p_{11}	−0.23	~ 0.20
p_{12}	−.03	~ .08
p_{13}	.02	~ 0
p_{14}	.00	—
p_{31}	−.04	~ 0
p_{33}	−.20	.252
p_{41}	.01	—
p_{44}	−.10	.085

All q_{ij} values in units of 10^{-13} cm^2/dyn.
All p_{ij} values are dimensionless.

Dixon has reported on some of the strain-optic constants of sapphire using a method which makes use of the acoustic scattering of a light beam [4]. Although the method does not permit the determination of the sign of the constants, the absolute values are listed in Table III for purposes of comparison with the present work, and it can be seen that there is fairly good agreement in the numerical values.

Caddes and Wilkinson have reported on the large photoelastic anisotropy of sapphire [5]. They have found the ratio of the elasto-optic constants $p_{33}/p_{13}\geq45$, which is consistent with our results. Our value of p_{13} compares favorably with the value, $p_{13}\approx0$ inferred by Davis and Vedam by analogy with the strain-optic constants of MgO [6, 20].

Pockels' phenomenological theory of photoelasticity assumes that the elastic deformations and not the stresses are primarily responsible for the changes in refractive index [21, 13]. It is interesting to note that for ruby (table 3) p_{11}, p_{12}, p_{31}, and p_{33} all show negative values. Of all the crystals studied thus far, only the covalent crystals Topaz, MgO and diamond exhibit negative values for $p_{hk}(h, k=1, 2, 3)$. In Topaz it is found that p_{11}, p_{22}, and p_{33} are all negative in value. MgO has negative values for both p_{11} and p_{12}, while diamond has a negative value for p_{11} only. All these crystals are noted for having strong interatomic bonding [13].

Mueller [22, 13] has developed a physical theory to explain the changes in the refractive index ellipsoid that take place when a solid is stressed. In this theory, calculations are made of the changes in the density, coulomb field, the lorentz-lorenz field, and the intrinsic polarizability of the scattering centers. The contribution of density is always positive and in most crystals exceeds the combined effect of the other three changes so that the p_{hk} are generally positive. The theory has been worked out for glasses and cubic crystals, but not for crystals of lower symmetry such as ruby (crystal class $\bar{3}$m) where the computations become extremely complicated. Although the individual contributions can not be calculated for ruby, it may be noted that the combination of the latter three changes outweighs the contribution due to change in density and, with the exception of p_{13}, the p_{hk} of ruby have negative values. Even with p_{13}, the positive numerical value is very small.

The photoelastic constants of calcite have been determined by Pockels [22, 13], and it is interesting to compare these data with the results on ruby because both crystals belong to class $\bar{3}$m. In both crystals the oxygen atoms are arranged in triangular groups per-

[2] These data also agree very well with the earlier measurements of Waxler and Weir on sapphire [15], when it is recognized that these investigators used Bridgman's compressibility data.

pendicular to the optic axis. However calcite has a true layer lattice, whereas Al_2O_3 possesses an isosthenic lattice in which the oxygen atoms are almost in hexagonal close packing. The elastic compliances of calcite are much greater than those of ruby [13]. This pronounced difference in the elastic compliances manifests itself in the photoelastic constants where it is found that the p_{hk} of calcite are all positive, and the p_{hk} of ruby are predominantly negative.

The authors are indebted to Harry B. Williams of the National Bureau of Standards for his great help in the preparation of specimens.

5. References

[1] Quelle, F. W., Appl. Opt. **5,** 633 (1966).
[2] Houston, T. W., Johnson, L. F., Kisliuk, P., and Walsh, D. J., J. Opt. Soc. Am. **53,** No. 11, 1286 (1963).
[3] Mandarino, J. A., Report from the Mineralogical Laboratory, Univ. of Michigan, Ann Arbor, Mich., cataloged by ASTIA as AD No. 146029.
[4] Dixon, R. W., J. Appl. Phys. **38,** 5149 (1967).
[5] Caddes, D. E., and Wilkinson, C. D. W., IEEE, J. Quantum Electron. QE 2, 330 (1966).
[6] Davis, T. A., and Vedam, K., J. Appl. Phys. **38,** 4555 (1967).
[7] Jeppesen, M. A., J. Opt. Soc. Am. **48,** No. 9, 629 (1958).
[8] Nye, J. F., Physical Properties of Crystals (Oxford Univ. Press, London, England, 1957).
[9] Wachtman, J. B., Jr., Tefft, W. E., Lam, D. G., Jr., and Stinchfield, R. P., Nat. Bur. Stand. (U.S.), **64A** (Phys. and Chem.), No. 3, 213–228 (May–June 1960).
[10] Malitson, I. H., and Dodge, M. J., NBS (data to be published).
[11] Peiser, H. S., Wachtman, J. B., Jr., and Dickson, R. W., Nat. Bur. Stand. (U.S.), **67A** (Phys. and Chem.) No. 5, 395–401 (Sept.–Oct. 1963).
[12] Curie, P., J. de Phys. 3 (3), 393 (1894).
[13] Krishnan, R. S., Progress in Crystal Physics, Volume **I** (Interscience Publishers, New York, London, 1958).
[14] Waxler, R. M., and Napolitano, A., J. Res. NBS **59,** No. 2, 121 (1957) RP2779.
[15] Waxler, R. M., and Weir, C. E., Nat. Bur. Stand. (U.S.), **69A** (Phys. and Chem.) No. 4, 325–333 (July–Aug. 1965).
[16] Saunders, J. B., J. Res. NBS 35, 157 (1945) RP1668.
[17] Wachtman, J. B., Jr., personal communication.
[18] Narasimhamurty, T. S., J. Opt. Soc. Am. **59,** No. 6, 682 (1968).
[19] Vedam, K., Proc. Ind. Acad. Sci. [A] **34,** 161 (1951).
[20] Vedam, K., and Schmidt, E. D. D., Phys. Rev. **146,** 548 (1966).
[21] Pockels, F., Wied. Ann. **37,** 151 (1889); Lehrbuch der Kristalloptic (B.6. Teubner, Leipzig and Berlin, 1906).
[22] Mueller, H., Phys. Rev. 47, 947 (1935).
[23] Pockels, F., Ann. Phys. (Leipzig) **11,** 726 (1903).

(Paper 74A2–592)